Tampere University

Ana Colucci Climent

STUDYING THE INTERACTION BETWEEN MACROPHAGES AND GLIOBLASTOMA CELLS IN 3D BRAIN MIMETIC HYDROGELS

Faculty of Medicine and Health Technology
Master's Thesis
September 2021

ABSTRACT

Ana Colucci Climent: Studying the Interaction Between Macrophages and Glioblastoma in 3D Brain Mimetic Hydrogels
Master's Thesis
Tampere University
Master's Program in Biomedical Technology
Supervisors: Oommen P Oommen, Vignesh Kumar Rangasami
Examiners: Heli Skottman, Oommen P Oommen
September 2021

Glioblastoma Multiforme (GM) is the cause of the majority of brain tumour deaths worldwide. Cancer cells take advantage of the tumour microenvironment (TME) and the cells that comprise it through complex signalling pathways in order to overcome our body's immune response allowing them to grow and proliferate in our system. Even if this is known, tumour microenvironments and their signalling are yet not fully understood.

To approach this problem, the behaviour of glioblastoma cells together with macrophages was studied in a 3D brain mimetic hydrogel, created with either carbohydrazide conjugated dopamine-modified hyaluronic acid (HADA-CDH) or carbohydrazide conjugated hyaluronic acid (HA-CDH), combined with aldehyde functionalized chondroitin sulphate (CS-Ald), components that are present in the brain's extracellular matrix. First, THP-1 and U87 MG cell lines were used as a model human macrophage cells and glioblastoma cells and were cultured together in the hydrogels to analyse their proliferation capabilities and gene expressions. After successfully establishing the protocol with the cell lines, we tested peripheral blood derived monocytes (PBMCs) derived macrophages and primary patient derived glioma cell (BT-13).

The results obtained during this study suggest that HA-CS hydrogels (HA-CDH combined with CS-Ald) sustained glioblastoma cells and macrophages better than HADA-CDH hydrogels. Moreover, it was shown that this 3D *in vitro* model gave reliable results with THP-1 and U87 MG cell lines, where M2-type macrophages nourished glioblastoma growth and proliferation. Nevertheless, the model did not show trustworthy enough results with the use of PBMC and BT-13 primary cells, therefore require further investigation.

Overall, this hydrogel platform opens a wide range of possible research areas and applications, such as disease modelling combined with drug analyses and testing, or the use of nanoparticles to target and silence specific glioblastoma genes.

Keywords: Glioblastoma Multiforme, Macrophages, 3D Hydrogel, Tumour Microenvironment

PREFACE

I would like to express my gratitude for Dr. Oommen P Oommen, Assistant Professor, Bioengineering and Nanomedicine Group, Faculty of Medicine and Health Technology, Tampere University, for his trust in me and for giving me the opportunity to carry out my thesis project in his research group.

I would like to thank Vignesh Kumar Rangasami for his continuous support and assistance during the project. I also thank Sumanta Samanta for offering help always when needed, and for the hydrogel materials used in the project.

Additionally, I want to thank Professor Susanna Miettinen, Adult Stem Cell Group, Faculty of Medicine and Health Technology, Tampere University, and Arjen Gebraad, Postdoctoral Research Fellow, for giving me access to the buffy coats and helping me with the handling of the PBMCs.

I would also thank Elina Lehtinen of the Faculty of Medicine and Health Technology, Tampere University, for her assistance and all the members of the Bioengineering and Nanomedicine Group for the help and the excellent environment to work in.

Tampere, 20 September 2021

Ana Colucci Climent

CONTENTS

LIST OF FIGURES

LIST OF SYMBOLS AND ABBREVIATIONS

ACTB	Beta-actin
BT-13	Patient-derived Glioblastoma Cells
CDH-1	E-Cadherin
CS-Ald	Aldehyde conjugated Chondroitin Sulphate
ECM	Extracellular Matrix
EDTA	Ethylenediaminetetraacetic acid
FBS	Foetal Bovine Serum
FGF	Recombinant Human Fibroblast Growth Factor
FGF-2	Fibroblast Growth Factor 2
GM-CSF	Granulocyte-Macrophage Colony-Stimulating Factor
GBM	Glioblastoma Multiforme
HA-CDH	Carbohydrazide conjugated Hyaluronic Acid
HADA-CDH	Carbohydrazide conjugated Dopamine-modified Hyaluronic Acid
IL-1RA	Interleukin-1 Receptor Antagonist
IL-4	Interleukin-4
IL-10	Interleukin-10
INFy	Interferon Gamma
LPS	Lipopolysaccharide
M-CSF	Macrophage Colony-Stimulating Factor
MMP-9	Matrix Metallopeptidase
MRC-1	Mannose Receptor C-type 1
M1	Classically Activated Macrophages
M2	Alternatively Activated Macrophages
NES	Nestin
PBMC	Peripheral Blood Mononuclear Cells
PBS	Phosphate-Buffered Saline
PMA	Phorbol 12-myristate 13-acetate
TAM	Tumour Associated Macrophages
THP-1	Human Acute Monocytic Leukaemia Cell Line
TME	Tumour Microenvironment
TNF	Tumour Necrosis Factor
U87 MG	Uppsala 87 Malignant Glioma Cells

1. INTRODUCTION

It is known that Glioblastoma Multiforme (GBM) is the most common malignant brain tumour, with a global incidence rate of <10 per 100,000 population (Taylor, Brzozowski, & Skelding, 2019). Cancer cells are characterized by several factors also known as Hall-marks of Cancer, one of which is sustaining proliferative signalling (Gutschner & Diederichs, 2012), which will allow the cancer cells to grow and develop in our body. The tumour microenvironment (TME) is composed mainly by tumour cells, tumour stromal cells, endothelial cells and immune cells. Complex signalling pathways between these will allow the tumour cells to control the TME, supporting and enhancing sustaining signalling for tumour growth and progression (Baghban, 2020).

It is already known that our immune system examines the body for any existing pathogen or tumour, and it does so by recognising the so known tumour-associated antigens (Pardoll, 2015). Macrophages comprise a major component of the immune system and immune responses. Some of their functions are to phagocyte and defend the body against foreign substances, and the regulation of T- and B-lymphocytes by activating them (Elhelu, 1983). The presence of factors such as interferon-gamma (IFNγ), polysaccharide (LPS) or tumour necrosis factor-alpha (TNFα), produced mainly by T helper 1 cells (TH1), will enhance the “classically activated” macrophages (M1) (H. W. Wang & Joyce, 2010), resulting in a strong inflammatory reaction (Troidl, 2009). However, T helper 2 cells (TH2) will stimulate the “alternatively activated” macrophages (M2) by the presence of factors such as interleukin 4 (IL-4), amongst others, enhancing tissue remodelling and neovascularization. Tumour associated macrophages (TAMs) are known to regulate and benefit tumour formation and metastasis, therefore acquiring the M2-type properties (H. W. Wang & Joyce, 2010).

Studying the crosstalk between tumour cells and TAMs, which promotes tumour cell growth, progression and invasion, is still a challenge. Recently, 3D *in vitro* models have been of huge interest when it comes to mimicking characteristics of tissues and even organs (Heinrich, 2019). In this way, a 3D *in vitro* model will more closely recapitulate the in vivo cellular interactions. More specifically, 3D hydrogel *in vitro* models have been an emerging prototype in medicine, for simple reasons such as the fact that animal models still show challenges regarding physiological similarities to humans and the ethical

concern about their use, and the fact that we are now advancing in human cell isolation and culturing (Liaw, Ji, & Guvendiren, 2018).

In this project we used two common extracellular matrix (ECM) compounds to mimic the brain microenvironment. Carbohydrazide conjugated hyaluronic acid (HA-CDH) or carbohydrazide conjugated on dopamine-modified hyaluronic acid (HADA-CDH), and aldehyde conjugated chondroitin sulphate (CS-Ald) were used. With both modified biomaterials we created a hydrazone crosslinked hydrogels, and cultured glioblastoma cells and macrophages, to be studied as a possible *in vitro* model.

2. LITERATURE REVIEW

2.1 The Human Brain

The human's brain main function is to control the body by simultaneously perceiving and processing information. Billions of neurons communicating together through synapses allow this to happen (Jawabri, 2020). The brain is mainly composed by the cerebrum, cerebellum and brainstem (Sachs, 1982). The cerebellum contributes to both motor and non-motor (cognitive) functions, and it plays a very important role in the timing and coordination of the human body (Desmond, 2019). The cerebrum, consisting of the cortex (grey matter) and an inner layer (white matter), has many different functions depending on the specific lobes into which it is divided: frontal, parietal, temporal and occipital) (Jawabri, 2020).

Two main types of cells comprise the nervous system: neurons and glial cells. The neurons' main function is to carry electrical signals along their axons and across synapses, but glial cells are known as supporting cells, as they protect and help neurons to carry out their function (Purves, 2001).

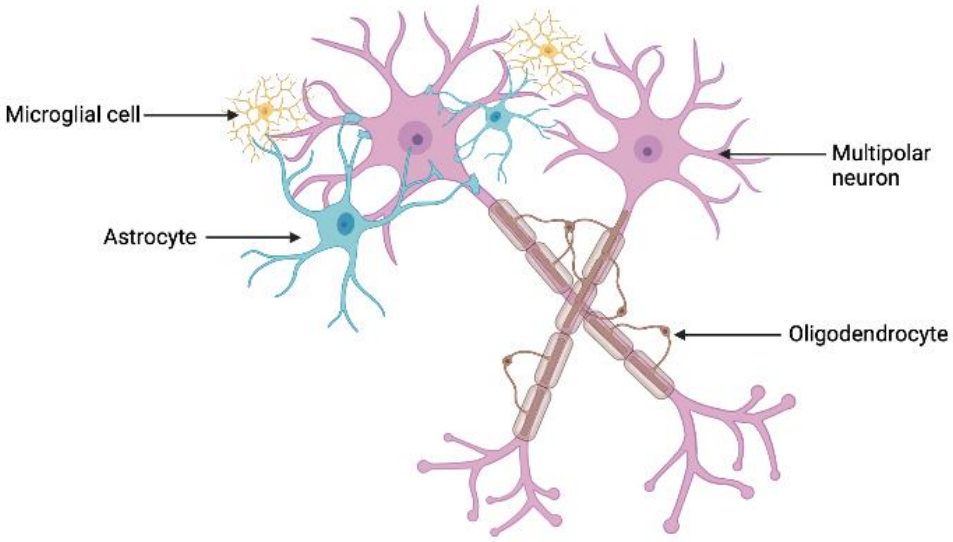

***Figure 1. Schematic view of neurons and glial cells**. Glial cells supporting neuron. The myelin sheath around the neuron's axon is formed by the oligodendrocytes. Nutrients are provided by astrocytes and provide structural support. Microglia cells get rid of pathogens and dead cells. (Modified from Rye, 2019).*

The main glial cells are astrocytes, oligodendrocytes, Schwann cells, microglial cells, ependymal cells and satellite cells, some of which can be observed in Figure 1. One of

the most important function of glial cells is the formation of myelin sheaths around the neuron's axons, thus providing a fast, electrical signal conduction. They also control the ion and neurotransmitter concentrations in the surrounding environment, essential for correct synapse function (Jessen, 2004). These cells are therefore playing a key role in the nervous system.

2.1.1 Brain Extracellular Matrix (ECM)

Most of the functions in the central nervous system (CNS) are dependent on the brain's extracellular matrix (ECM). Some of which include cell support, electrical impulse transmissions allowing communication between cells, or growth regulation (Suttkus, Morawski, & Arendt, 2016). The main components of the ECM that assist in these events to take place – amongst others – are, for example, tenascin-C, neurocan and hyaluronan (Rauch, 2004). Versican, aggrecan and glial HA-binding proteins (GHAP) are known to bind HA and take part in the brain's development (Bignami, Hosley, & Dahl, 1993). Because of its high variety of functions, HA is widely known in brain-related studies, and so is the contribution of tenascin-C in brain morphology, but neurocans – also known as chondroitin sulphate proteoglycans – have been seen to take part in important barrier functions (Rauch, 2004). Neurocans interact with growth and mobility factors (i.e. FGF-2), structural and matrix proteins (i.e. tenascin-C), neural cell adhesion molecules (i.e. N-CAM) and other molecules (i.e. GPI-linked membrane molecules) (Rauch, Feng, & Zhou, 2001). Synaptic plasticity and performance is also highly regulated by neuromodulators, such as dopamine (DA) (Mitlöhner et al., 2020). The brain ECM is such an important component in the study of the brain's development and mechanisms, that it has to be taken into consideration when carrying out studies with brain cells.

2.2 Glioblastoma Multiforme (GBM)

Primary brain tumours are known as gliomas, and their classification depends on the origin of the cell type in question. Some examples include astrocytic tumours, oligodendrogliomas or ependymomas amongst others. The most malignant and frequent type of primary astrocytoma is glioblastoma multiforme (GBM), which accounts for more than 60% of adult brain tumours (Hanif, 2017).

GBM consists mainly of a group of tumours both genetically and phenotypically heterogeneous. *De novo* glioblastoma multiforme tumours are developed from glial cells by a process known as multistep tumorigenesis, and accounts for 90% of the cases (Urbanska, 2014). The prognosis of GBM patients is very poor, of about one-year survival rate in only 37.2% of the cases, being around ten months the median survival. As

the majority of the human cancers, GMB is divided into different types according to the mutation state of isocitrate dehydrogenase 1 and 2 (IDH1 and IDH2), however treatments remain the same for all patients despite the different tumour classifications (Taylor, 2019). Nonetheless, survival rate has significantly improved over the last century with the advances of radiotherapy and chemotherapy (Zhang, 2019).

2.3 Tumour Microenvironment and Immune Cells

Although there is already a wide knowledge about cancer, the main reasons for cancer formation are still not completely understood. This gap of understanding also includes the characteristics of both the cellular and noncellular components that help the tumours to grow and expand. These components altogether form the tumour microenvironment (TME) (M. Wang, 2017). The tumour cells found in the TME are known to communicate through complex signalling pathways with both cellular and noncellular components and control them for the own benefit of the tumour. The consequence of this crosstalk is therefore the tumour growth and expansion, as well as resistance to therapy or multi-drug resistance (Baghban, 2020).

One component of the TME is endothelial cells, which help tumour development and enhance tumour cell protection against the body's immune system. They also form branching angiogenic vessels to support the tumour with the required nutrients to grow (Siemann, 2010). Additionally, cytokines, growth factors or chemokines are secreted by tumour cells, which will consequently attract immune cells, the major TME component (Barriga, 2019). The main immune cell type in the TME is tumour-associated macrophages (TAMs). These mainly express anti-inflammatory markers such as interleukin 10 (IL-10) and IL-1 receptor alpha (IL-1Ra), which highly contribute to tumour development, and therefore acquire the M2-like macrophage characteristics. Moreover, these TAMs can recruit even more monocytes to be polarized into more M2-phenotype macrophages. In addition, they also promote neovascularization. The three major roles that TAMs play in the TME are angiogenesis, chronic inflammation and immune suppression (J. Wang, 2019). Another TME component is comprised by fibroblasts, which allow the tumour cells to migrate into the bloodstream from the primary tumour location, therefore enhancing metastasis (Siemann, 2010).

2.4 Three-Dimensional Cell Cultures

For many years, two-dimensional (2D) cell cultures have been the basic study methods in laboratories for research purposes. These monolayers of cells have highly helped

studying and discovering many cell behaviours and characteristics, but over the years its limitations have been rapidly increasing. It is now well known that components in the *in vivo* environment are surrounded and affected by many factors, more like in a three-dimensional (3D) way (Edmondson, 2014), as seen in Figure 2.

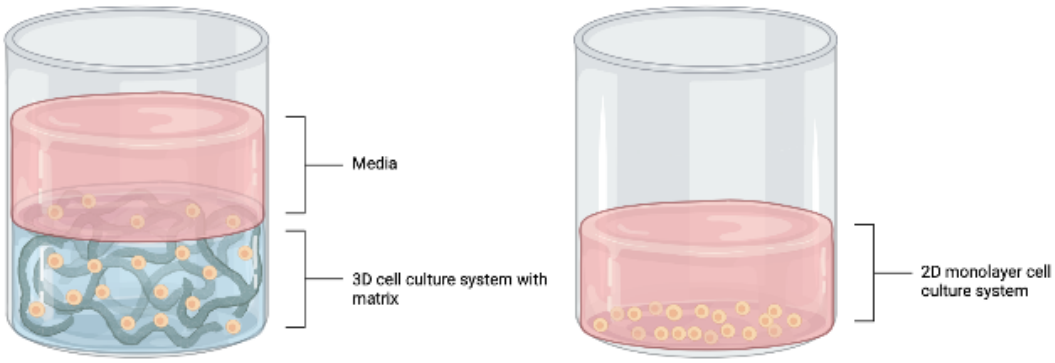

Figure 2. *Schematic diagrams of **A)** two-dimensional and **B)** three-dimensional cell cultures (Modified from Chaicharoenaudomrung, 2019).*

It is cheaper, easier and faster to carry out studies in 2D, but the differences in cell-to-cell or cell-to-matrix interactions, morphological characteristics, cell signalling and other factors may contribute to misleading results and conclusions (Chaicharoenaudomrung, 2019).

In the 1970s the first three-dimensional culture was made by Hamburg and Salmon in soft agar solution. Nowadays, these cultures can be carried out in suspension cultures with non-adherent surfaces, in gel-like substances, or in scaffolds (Kapałczyńska, 2018). One way to culture cells in a 3D fashion is by the formation of spheroids, which occur in suspension when cells tend to self-aggregate together, and is also a natural process occurring for example during embryogenesis or organogenesis (Ryu, 2019). Another way is by the so known organoids, which, deriving from stem cells or primary tissues, they are cultured in a controlled and defined environment, and will self-organize into a structure mimicking those characteristics of either a healthy or diseased model. These organoids will recapitulate many characteristics of the specific tissue, and they can also be propagated (Lehmann, 2019). A recent technique with high interest for 3D culturing is the organ-on-a-chip technology (OOC). It is composed by a compartment that has been engineered to control and study how drugs or other stimuli affect cell behaviour. It is a challenging method as it combines the knowledge in microfluidics, biomimetic tissues

and monitoring systems, but it closely mimics the *in vivo* environment (Jodat, 2019). Together with this method, the popularity of 3D bioprinting in research has been increasing up to date. By the use of viable cells, together with biomaterials and biological molecules, it is possible to design scaffolds which provide stability and promote cell growth, in order to mimic body tissues or organs, which makes it possible to study the cell's behaviour. It is even possible to add a vascularization system to the structure, which will provide the cells with oxygen and nutrients, thus reinforcing the *in vivo* microenvironment (Kačarević, 2018). Having all these new, high technology methods opens a lot of new possibilities in research. The fact that these methods are of new, high technology, sometimes makes it a challenge to have access to in laboratories, so experimental set-ups by the use of hydrogel scaffolds are more common and cheaper to be used. These are commonly composed of hydrophilic polymers that crosslink and create 3D networks, mimicking the ECM, and therefore creating an environment for cells to grow (El-Sherbiny & Yacoub, 2013).

2.5 *In Vitro* Brain Cell Culture Models

Many brain disorders such as Alzheimer's disease, schizophrenia or Parkinson's disease have been modelled in the laboratory for research purposes, but still, studying the human brain by recapitulating its complicated architecture is not easy. Even so, there are several *in vitro* brain cell culture models that have been used to study specific parts and characteristics of the brain.

Examples of 3D cellular models to mimic the complexity of the human brain include, for example, organotypic brain slice cultures to study physiology, development and even electrophysiology, for instance in the hippocampus, as it is an area of the brain where neural loss or other pathologies are most common (Croft, Futch, Moore, & Golde, 2019). Some of the neurological diseases have been studied by the use of organs-on-chip models, where microfluidics are put in use to control the cellular microenvironment (Jorfi, D'Avanzo, Kim, & Irimia, 2018). These microfluidic systems are categorized depending on the materials used, which can be glass/silicon, polymers or paper (XiuJun (James) Li, Alejandra V. Valadez, Peng Zuo, 2012). Neurospheroids have also been developed from neural cells that assembly themselves into spheroid structures in culture (Dingle et al., 2015). This method is used for drug screening or disease modelling, but the high sensitivity of the neurospheroids makes it challenging when it comes to reproducibility (Jorfi et al., 2018). Cerebral organoids are another example of brain cell culture models to study brain disorders such as microencephaly, where PSCs from human neural tissue are cultured in a bioreactor (Bershteyn & Kriegstein, 2013). The blood-brain barrier (BBB)

is a very much studied area of the brain because of its high importance, and many of these *in vitro* models have been applied to recapitulate its functions (Wilhelm, 2011).

Mimicking the ECM is also important when it comes to reproducing brain cell culture models. Both natural (i.e. collagen and Matrigel) and synthetic (i.e. polymers and peptides) forms have been used in laboratories (Jorfi et al., 2018). The reason why sometimes synthetic matrices, such as poly ethylene glycol (PEG), have been used is mainly because of the variations from batch-to-batch and not always perfectly-defined compositions of natural matrices (Jorfi et al., 2018). The obvious advantage of using natural matrices is the fact that they are present in the *in vivo* microenvironment and will provide the models with the real biological properties of the ECM (Jorfi et al., 2018). Such natural matrices can be composed for example by hyaluronic acid (HA), a polysaccharide used, for example, in tissue regeneration or wound healing applications (Tang et al., 2020).

The use of this wide variety of 3D models to recapitulate a tumour and its environment (TME) has allowed us to study how cells behave in terms of, for example, growth and invasiveness, and their behaviour towards drugs or chemo/radiotherapy, but challenges are still to be overcome. The TME is not always constant, but its composition is varying as the tumour progresses, and this is still a big obstacle, as well as being able to recapitulate the heterogeneity of tumours (Blanco-Fernandez, 2021).

2.6 Hydrogels as *In Vitro* Cell Culture Models

Over the years scientists have shown an increased interest in the use of biomaterials for research purposes as they have shown a high biocompatibility, amongst other properties (Mantha, Pillai, Khayambashi, Upadhyay, & Zhang, 2019). Biomaterials have been described as substances that have been engineered for medical purposes to interact with biological systems, which therefore give the possibility to be used as cell culture systems, scaffolds or tissue engineering (Catoira, Fusaro, Di Francesco, Ramella, & Boccafoschi, 2019). Moreover, hydrogels comprise a huge part of the biomaterials used in research over the last years.

Hydrogels are three-dimensional (3D) polymeric networks, which can be composed by natural or synthetic polymers (Lee & Kim, 2018). Synthetic hydrogels, such as polyacrylamide (PAA) or polyethylene glycol (PEG), have good stability and mechanical properties, which make them reproducible and controllable in the laboratory (Aswathy, Narendrakumar, & Manjubala, 2020). However, natural hydrogels composed by collagen, gelatin or hyaluronic acid (HA), mimic the brain ECM that we aimed to develop as

a hydrogel in a more desirable way. Additionally, they are biocompatible, therefore having low cytotoxicity towards cells, and are biodegradable, which allows them to be used for biomedical applications (Catoira et al., 2019). It is for these reasons that we carried out our study with the use of carbohydrazide conjugated hyaluronic acid (HA-CDH) or carbohydrazide conjugated on dopamine-modified hyaluronic acid (HADA-CDH), and aldehyde conjugated chondroitin sulphate (CS-Ald).

2.6.1 Hyaluronic Acid (HA)

Hyaluronic acid (HA) is a glycosaminoglycan (GAG) with repeating disaccharide units of glucuronate and *N*-acetyl glucosamine (Figure 3), it is known to take part in wound healing and development, and it can be find in several parts of the body such as the skin, cartilage, and especially in the brain (Aswathy et al., 2020). Some other properties include hydrophilia, non-adhesiveness and biodegradability (Catoira et al., 2019).

This biopolymer comprises the main structural component of the brain's ECM, which is one of the main reasons why it was chosen for this study (Bignami et al., 1993). We modified HA by combining it with carbohydrazide (CDH), a compound that has been found useful against autoimmune and inflammatory diseases, respiratory diseases, cardiovascular diseases or even tumours (Mansour, Eid, & Khalil, 2003).

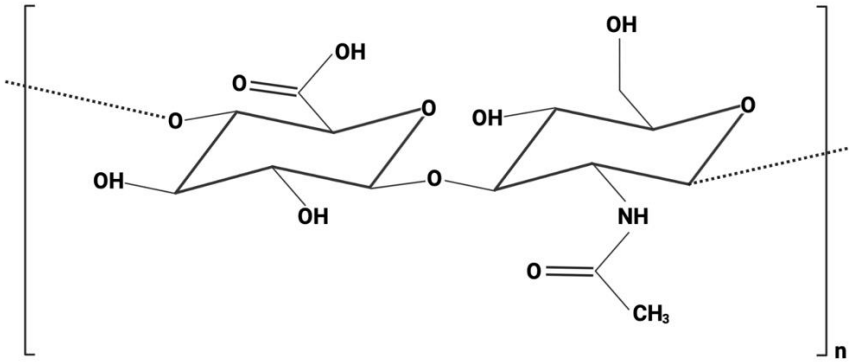

Figure 3. Chemical structure of hyaluronic acid (HA) *(Modified from Fallacara, Baldini, Manfredini, & Vertuani, 2018).*

2.6.2 Chondroitin Sulphate (CS)

Chondroitin sulphate (CS) is a sulphated GAG with repeating disaccharide units of *N*-acetylgalactosamine (Figure 4), it is very commonly found in connective tissues like bone, cartilage or skin, and it plays an important role in resistance and elasticity (Henrotin, Mathy, Sanchez, & Lambert, 2010). It biologically takes part in cell adhesion,

division, differentiation and morphogenesis, and it is also involved in infection, inflammation and wound repair (Volpi, 2019).

We created aldehyde conjugated chondroitin sulphate (CS-Ald). Aldehydes have been used to conjugate polymers, as they can be used for a wide range of applications, such as regenerative medicine, developing of adhesive glues and for hydrogels, amongst others. As for the project, we combined aldehyde together with CS normally present in the ECM so that biocompatibility is enhanced (Varghese, Wang, Oommen, & Yan, 2013).

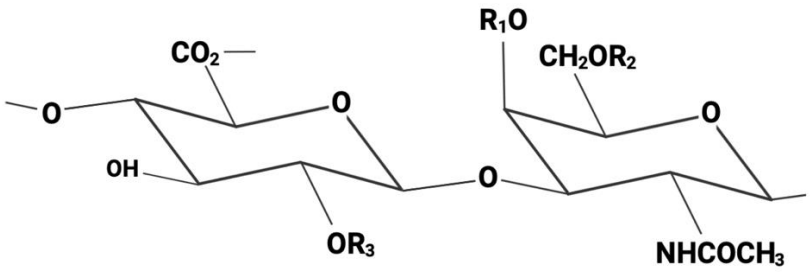

***Figure 4. Chemical structure of chondroitin sulphate (CS)**, where R_1 = R_2 = R_3 = H: non-sulfated chondroitin. R_1 = SO_3^-; R_2 = R_3 = H: chondroitin-4-sulfate; R_1 = R_3 = SO_3^-; R_2 = H: chondroitin-2,4-disulfate; R_2 = SO_3–; R_1 = R_3 = H: chondroitin-6-sulfate; R_2 = R_3 = SO_3^-; R_1 = H: chondroitin-2,6-disulfate; R_1 = R_2 = SO_3^-; R_3 = H: chondroitin-4,6-disulfate; R_1 = R_2 = R_3 = SO_3^-: trisulfated chondroitin (Modified from Volpi, 2019).*

3. OBJECTIVES

Engineering a tumour microenvironment that mimics the tumour and its surroundings is an important research area. In this project, we will tailor a brain mimetic 3D scaffold and culture human monocytes, or macrophages to evaluate the crosstalk between the immune cells and glioma cells.

We anticipate that when the monocytes are differentiated into the M2 or TAM-like phenotype, there will be increased paracrine signalling between the tumour cells and macrophages as well as intratumoral interactions which would stimulate the expression of tumour promoting genes and tumor invasiveness, thereby proving the validity of our model. On the other hand, we believe that if we polarize the TAM-like M2 macrophages to proinflammatory M1-type, it would reduce the invasiveness and EMT transition and reduce the expression of tumour promoting genes.

4. MATERIALS & METHODS

The materials and workflow of the study are described in this chapter.

Human acute monocytic leukaemia cell line (THP-1), peripheral blood mononuclear cells (PBMCs), Uppsala-87 malignant glioma cells (U87 MG) and patient derived BT-13 glioblastoma cells were used for this experiment.

4.1 Cell Culturing and Splitting

Cell culturing and splitting of the cells was carried out in the cell culture laboratory parallel to the main study. The U87 MG cells were cultured in complete medium (DMEM 1x (Gibco, #31885-023) containing 10% foetal bovine serum (FBS, Gibco, #10270-106) and 1% Penicillin-Streptomycin (10,000 U/mL) (Gibco, #15140122)). U87 MG cells were cultured in 175 cm^2 flasks together with 20 mL of the prepared DMEM and incubated at 37°C and 5% CO_2. The THP-1 monocytic cell line was cultured in complete medium (RPMI 1x (Gibco, #21875-034) containing 10% foetal bovine serum (FBS) and 1% Penicillin-Streptomycin (10,000 U/mL)). The THP-1 monocytic cell line was cultured in 25 cm^2 flasks together with 10 mL of the prepared RPMI each and incubated at 37°C and 5% CO_2. The FBS was used as a growth supplement for the cell culture. The BT-13 glioblastoma cells were cultured in complete medium (DMEM/F-12 no glutamine (Gibco, #10565-018) containing 2% B27 Serum Free Supplement 50x (Gibco, #17504044) and 0,2% Penicillin-Streptomycin (10,000 U/mL) (Gibco, #15140122)). Finally, 10 µL of Recombinant Human Fibroblast Growth Factor (FGF; 10 µg/mL) (Peprotech AF-100-18B) was added. BT-13 cells were cultured in 25 cm^2 flasks together with 10 mL of the prepared DMEM/F-12 and incubated at 37°C and 5% CO_2.

Cell splitting was carried out approximately every two days according to the cell confluency level. The flasks were observed under a microscope to check the cells' growth state. For U87 MG, the old medium was removed from the flask, and it was carefully washed with 3-5 mL of phosphate-buffered saline (PBS, Gibco, #1877586). The PBS was removed and 3 mL of Trypsin (TrypLE, Gibco, #12604-013) or Ethylenediaminetetraacetic acid solution (EDTA, Sigma-Aldrich, #E8008) was added to loosen the cells from the flask surface. The flask was then observed under the microscope to check that the cells had not been washed away, followed by an incubation of 5-7 minutes at 37°C. To stop the trypsinization process, 7 mL of complete DMEM was added. After this, the cells were centrifuged at 1200 rpm for 5 mins. A pellet containing the cells was formed, and

the supernatant was discarded. The pellet was resuspended in 1 mL of complete DMEM. The cells were counted with Countess™ II Automated Cell Counter (Invitrogen) by mixing 10 µL of Tryphan Blue (Sigma-Aldrich, T8154) and 10 µL of the cell suspension. Finally, 20 mL of complete DMEM and a desired amount of the cell suspension was added to a new 175 cm^2 flask. The newly prepared flask was incubated in 5% CO_2 at 37°C. For THP-1 monocytic cell line Trypsin or EDTA were not necessary as the cells grew in suspension. The cultures from both 25 cm^2 flasks were centrifuged at 1200 rpm for 5 mins. The supernatant was discarded, and the pellet was resuspended in 1 mL of complete RPMI. The cells were counted with Countess™ II Automated Cell Counter (Invitrogen) by mixing 10 µL of Tryphan Blue and 10 µL of the cell suspension. Finally, two new 25 cm^2 flasks were prepared with 10 mL of complete RPMI each and a desired amount of the cell suspension. The newly prepared flasks were incubated in 5% CO_2 at 37°C. For BT-13 cells Trypsin or EDTA were not necessary as the cells grew in suspension. The cells were centrifuged at 1200 rpm for 5 mins. The supernatant was discarded, and cells were resuspended and washed with 5 mL of PBS. Cells were centrifuged at 1200 rpm for 5 mins, supernatant was removed and 1 mL of Accutase solution (Sigma-Aldrich, #SLCG0476). Cells were pipetted up and down to dissociate spheroids, followed by water bath incubation at 37°C. An additional 5 mL of DMEM/F-12 was added, and cells were centrifuged at 1200 rpm for 5 mins. Supernatant was removed and cells were resuspended in 6 mL of fresh DMEM/F-12. Only 3 mL of the cell suspension was added to a new 25 cm^2 flask together with 7 mL of DMEM/F-12 and 10 µL FGF.

4.2 Priming, Polarization and Activation of Macrophages

The human THP-1 monocytes were primed with 50 ng/mL PMA (phorbol 12-myristate 13-acetate) (Sigma-Aldrich, #MKCC8966) and incubated for 24 h in 5% CO_2 at 37°C to bring them to M0 phenotype. Then, interleukin 4 (IL-4) (30 ng/mL) (Sigma-Aldrich, #1406240B) was administered to polarize the M0 into M2-type macrophages. Once differentiated, the cells would become adherent, and ready to use in the experiment.

The PBMCs were first extracted from a buffy coat (Tays Central Hospital, Tampere, A+ blood sample, 034380) (≈$125{,}5 \times 10^6$ cells) following a PBMC isolation protocol and plated in 4 Petri Dishes (≈31×10^6 cells/dish) together with basal RPMI and incubated for 3 h in 5% CO_2 at 37°C. Each Petri Dish was then washed with warm PBS, and 10 mL of the specific polarization media was added per dish. The polarization reagent used to obtain M1-type cells was granulocyte-macrophage colony-stimulating factor (GM-CSF; 50 ng/mL), and the reagent to obtain M2-type cells was macrophage colony-stimulating factor (M-CSF; 50 ng/mL). After this, the cells were incubated for 6 days at 37°C in 5% CO_2.

The polarization media was then removed from the Petri Dishes, and 10 mL of activation media was added per dish. The M1-type macrophage activation media contained Interferon Gamma (INFy; 50 ng/mL), lipopolysaccharide (LPS; 10 ng/mL) and GM-CSF (50 ng/mL). The M2-type macrophage activation media contained IL-4 (20 ng/mL) and M-CSF (50 ng/mL). The Petri Dishes containing M2-type macrophages were incubated for 2 days, and the Petri Dishes containing M1-type macrophages were incubated for 5 days.

4.3 Hydrogel Preparation

For this experiment, either carbohydrazide conjugated hyaluronic acid (HA-CDH) or carbohydrazide conjugated on dopamine-modified hyaluronic acid (HADA-CDH) were combined with aldehyde conjugated chondroitin sulphate (CS-Ald) by chemical crosslinking, which consists on mainly covalent bonds creating permanent junctions (Zhu & Marchant, 2011). They were all dissolved to a concentration of 14 mg/mL, and equal volumes of carbohydrazide and aldehyde derivatives were used to make the hydrogels. Before combining the materials, HA-CDH or HADA-CDH had to be dissolved in 10% sucrose solution, while CS-Ald was dissolved in PBS. The materials were sterilized under UV light for 30 minutes prior to the experiment.

4.4 Experimental Setting and Cell Plating

The first set of experiments were carried out by using the U87 MG glioblastoma cells and THP-1 monocytic cells. The last set of experiments were carried out using BT-13 glioblastoma cells and patient derived PBMCs. For the experiments, 48-well plates were used. A total of three different groups were analysed in the hydrogels: macrophages control group; glioblastoma cells control group; glioblastoma microenvironment group (GME), having four parallels (replicas) each, as seen in Figure 5.

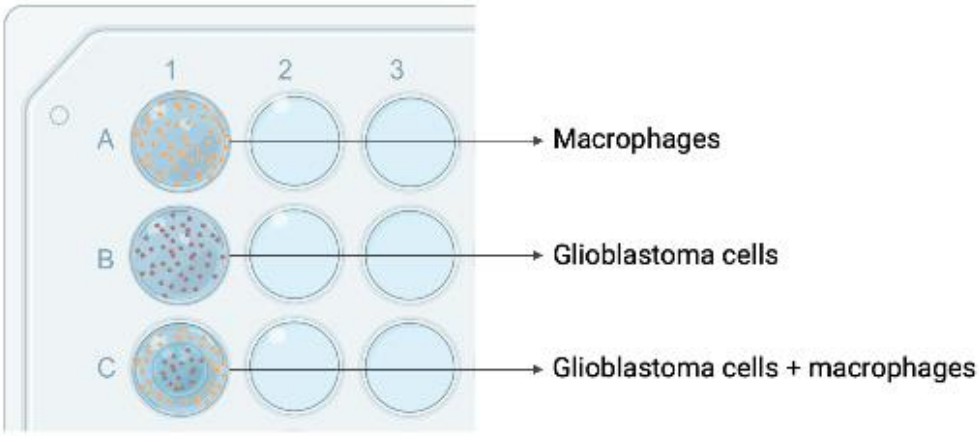

Figure 5. Schematic figure of the experimental setting in a 48-well plate. *Three different hydrogel groups are shown to be analysed: glioblastoma cells control group (top); macrophages control group (middle); glioblastoma microenvironment group (bottom). Each of the groups having 4 replicas. Created with BioRender.com*

For the control groups, 800 000 cells were plated in 200 µL hydrogels (Figure 6A). For the GME group, 800 000 macrophages were plated in 200 µL hydrogels, and 200 000 glioblastoma cells were plated in 50 µL hydrogels (Figure 6B).

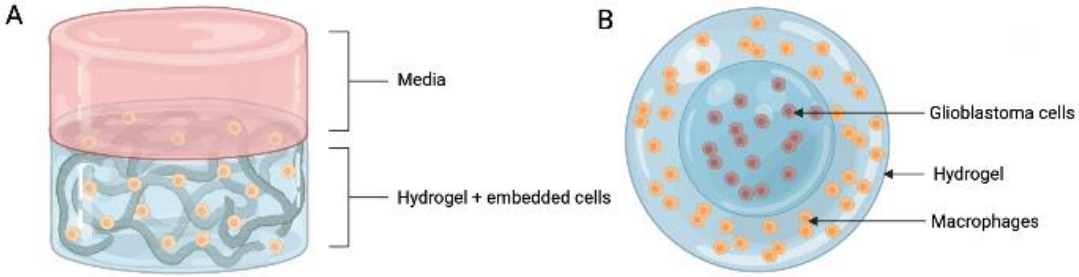

Figure 6. Schematic view of the hydrogel experimental setup. A) *Representation of one of the wells in the 48-well plate, where the hydrogel (V: 200 µL) is formed at the bottom, and the media (V: 500 µL) is added on top.* ***B)*** *Top view of one of the wells in the 48-well plate of the GME group ($V_{GLIOBLASTOMA}$: 50 µL; $V_{MACROPHAGES}$: 200 µL). Created with BioRender.com*

4.4.1 Glioblastoma and Macrophage control groups

To plate the cells together with the hydrogels in the plate wells, first the cells were counted individually. Once the desired number of cells was obtained, they were centrifuged at 1200 rpm for 5 mins. A total of 100 µL/well of CS-Ald was first added in the four

required wells. The pelleted cells were resuspended in 400 µL HADA-CDH or HA-CDH. Finally, 100 µL of the HADA-CDH or HA-CDH and cell mix was transferred to the wells containing 100 µL CS-Ald. Mixing with the pipette tip was necessary for a homogeneous mix of all the materials.

4.4.2 Glioblastoma Microenvironment Group (GME)

Once the desired number of macrophages was obtained, they were centrifuged at 1200 rpm for 5 mins. A total of 100 µL/well of CS-Ald was first plated in the four required wells. The pelleted cells were resuspended in 400 µL HADA-CDH or HA-CDH. Finally, 100 µL of the HADA-CDH or HA-CDH and macrophage mix was transferred to the wells containing 100 µL CS-Ald. Mixing with the pipette tip was necessary for a homogeneous mix of all the materials. The hydrogels were incubated for 30 minutes in 5% CO_2 at 37°C. Then, a gap in the shape of a circle was made in the centre of the gel with the use of a pipette tip. Once the desired number of glioblastoma cells was obtained, they were centrifuged at 1200 rpm for 5 mins. A total of 25 µL/well of CS-Ald was first added to the gap created in the four required wells. The pelleted cells were resuspended in 100 µL HADA-CDH or HA-CDH. Finally, 25 µL of the HADA-CDH or HA-CDH and glioblastoma cell mix was transferred to the wells containing 100 µL CS-Ald.

Once the hydrogels were cured, 500 µL of the corresponding medium was added to the wells. The 48-well plates with the hydrogels were incubated in 5% CO_2 at 37°C, and analysed after 1, 7 and 14-day timepoints. Media was changed every two days.

4.5 Cell Characterization Methods

Several methods were used to characterize cells on different timepoints starting from the experiment day.

4.5.1 Live/Dead Assay

This assay was performed to determine the percentage of live cells in the hydrogels. This is also known as fluorescence cell viability assay, where Calcein-AM stains live cells green, and Ethidium Bromide stains dead cells red (Neri, Mariani, Meneghetti, Cattini, & Facchini, 2001). To check the cell viability LIVE/DEAD staining (Viability/Cytotoxicity Kit for mammalian cells, Molecular Probes, USA) was carried out followed by analysis using a fluorescence microscope. First, medium was removed from the wells, and 500 µL Live/Dead staining solution containing 1 µL/mL Calcein-AM and 0,5 µL/mL Ethidium Bromide in 1X PBS was added. The plates where incubated in 5% CO_2 at 37°C for 2 hours.

After incubation, images were then taken with Nikon Eclipse Ts 2 fluorescence microscope on a 10x objective. The images obtained were post-processed using Nikon NIS Viewer and ImageJ softwares.

4.5.2 PrestoBlue Assay

PrestoBlue is based on a chemical known as resazurin, which is normally a blue, non-fluorescent and membrane permeable compound which will be reduced into the resorufin form when entering the cell, emitting fluorescence that can be quantified to determine the cell viability (Lall, Henley-Smith, De Canha, Oosthuizen, & Berrington, 2013).

A working solution of 10% PrestoBlue (Thermo Fisher Scientific) diluted in PBS was placed on top of the hydrogels after removing the medium and was incubated for 8 hours in 5% CO_2 at 37°C in the dark. After incubation, the solution was transferred into a 96-well plate to measure the florescence signal at excitation/emission wavelengths 560/590 with Perkin Elmer multilabel counter plate reader.

4.5.3 Gene Expression Analysis

Gene expression analysis was performed to study more closely the interaction between the glioma cells and macrophages. The expression level of several brain-specific (glioma) and immune-specific (macrophages) genes were measured and compared at the different experimental timepoints. The upregulation or downregulation of genes is affected by the environment which surrounds the cells, together with other factors. It is possible to quantify the level of gene expression and the fold change of these gene expressions of cells exposed to different environments to analyse their different behaviour (Krebs, J.E., E.S. Goldstein, 2017).

First, RNA extraction was carried out, followed by cDNA synthesis from the extracted RNA, finishing with a quantitative reverse transcription polymerase chain reaction (qRT-PCR) for gene expression quantification.

RNA extraction

RNA extraction follows the steps of isolation and purification of RNA (Tan & Yiap, 2009). After each experimental timepoint, RNA samples were collected from each hydrogel group separately (including the macrophages and glioblastoma cells from the GME groups). The hydrogels were mechanically broken down with the use of a spatula, and hydrogel disintegration was enhanced by dissolving in PBS. The solution was filtered through a cell strainer to remove as much of the hydrogel materials as possible, and

isolate the cells, followed by centrifugation and discarding of supernatant. RNA samples were then extracted and purified using RNeasy Mini Kit (Qiagen). The cells were first lysed with a cell lysis buffer, and filtrated through gDNA eliminator column, followed by several washes to eliminate contaminants, such as proteins and lipids. The RNA concentration was measured (ng/µL) with NanoDrop (ND-1000, Thermo Fisher Scientific Inc., USA).

cDNA synthesis

Same RNA concentrations were taken from each of the measured samples in order to get as consistent results as possible. RNA was mixed with water to make up to 10 µL volume, and to each sample ds-DNase and DNase buffer from cDNA synthesis kit (Thermo Fisher Scientific) was added. After 5 minutes, 5X Reaction Mix, reverse transcriptase enzyme and water from the kit were added. A thermocycler was used to then carry out the cDNA synthesis.

Quantitative reverse transcription polymerase chain reaction (qRT-PCR)

TaqMan Fast Advanced Master Mix (Thermo Fisher Scientific), water and primers were added together with the cDNA samples. This mix was then processed by Bio-Rad CFX96 Real-time PCR machine, to quantify gene expression. The cycle threshold (Ct) values, which shows the first sensed signal indicating the first PCR cycle at which it was detected (Ade et al., 2021), were later on analysed following the $\Delta\Delta C_q$ calculation method to obtain the relative gene expression values together with knockdown percentage for each of the genes of interest (Haimes & Kelley, 2010).

A list of the analysed genes in the experiment are shown in Table 1.

Table 1. List of the analysed genes by qRT-PCR. *ACTB used as endogenous gene.*

Gene	Gene Product	TaqMan ID
ACTB	Beta-actin	Hs01060665
FGF-2	Fibroblast growth factor 2	Hs00266645
MMP-9	Matrix metallopeptidase	Hs00957562
TNF	Tumour necrosis factor	Hs00174128
IL-1RA	Interleukin-1 receptor antagonist	Hs00893626
IL-10	Interleukin-10	Hs00961622
MRC-1	Mannose receptor C-type 1	Hs00267207
CDH-1	E-cadherin	Hs01023895
NES	Nestin	Hs04187831

5. RESULTS AND DISCUSSION

5.1 Hydrogel Optimisation

For the first set of experiments, THP-1 cells were polarized and activated into M2-type macrophages, and U87 MG cells were used as a model glioblastoma cell. To test the efficiency and the biocompatibility of the hydrogels, Live/Dead and PrestoBlue assays were carried out on days 1 and 7 timepoints.

We first tested the biocompatibility of HA-CS composite gels, grafted with dopamine (DA) groups (HA-DACS gels). As mentioned earlier, dopamine is an important neuromodulator present in the brain's ECM (Mitlöhner et al., 2020). Additionally, dopamine shows to improve hydrogel stability in medium, with a high swelling ratio, mimicking the *in vivo* microenvironment (Koivusalo et al., 2019). The THP-1 and the U87 MG cells were cultured in separate hydrogels as mentioned above. Around 800 000 cells were encapsulated in these hydrogels and were cultured for a period of 1 and 7 days. At these time points the gels were analysed using the Live/Dead and PrestoBlue assays. It was interesting to note that there was a high number of dead THP-1 and U87 MG cells in day 1 from the Live/Dead assay. One probable reason for the high number of dead cells in the U87 MG groups could be due to the presence of dopamine in the hydrogel. Dopamine is known to inhibit the proliferation rates of the tumour cells, as it has shown to affect apoptosis and tumour angiogenesis in cancer cell lines, causing a decrease in tumour size (X. Zhang, Liu, Liao, & Zhao, 2017). In the case of the THP-1 cells, we believe that treatment with EDTA (2mM) for 30 minutes could have been the main cause of the cell death, as we observed high number of cell death even before the cells were encapsulated in the gels. The PrestoBlue assay also confirmed the observations seen in the Live/Dead assays (Figure 7).

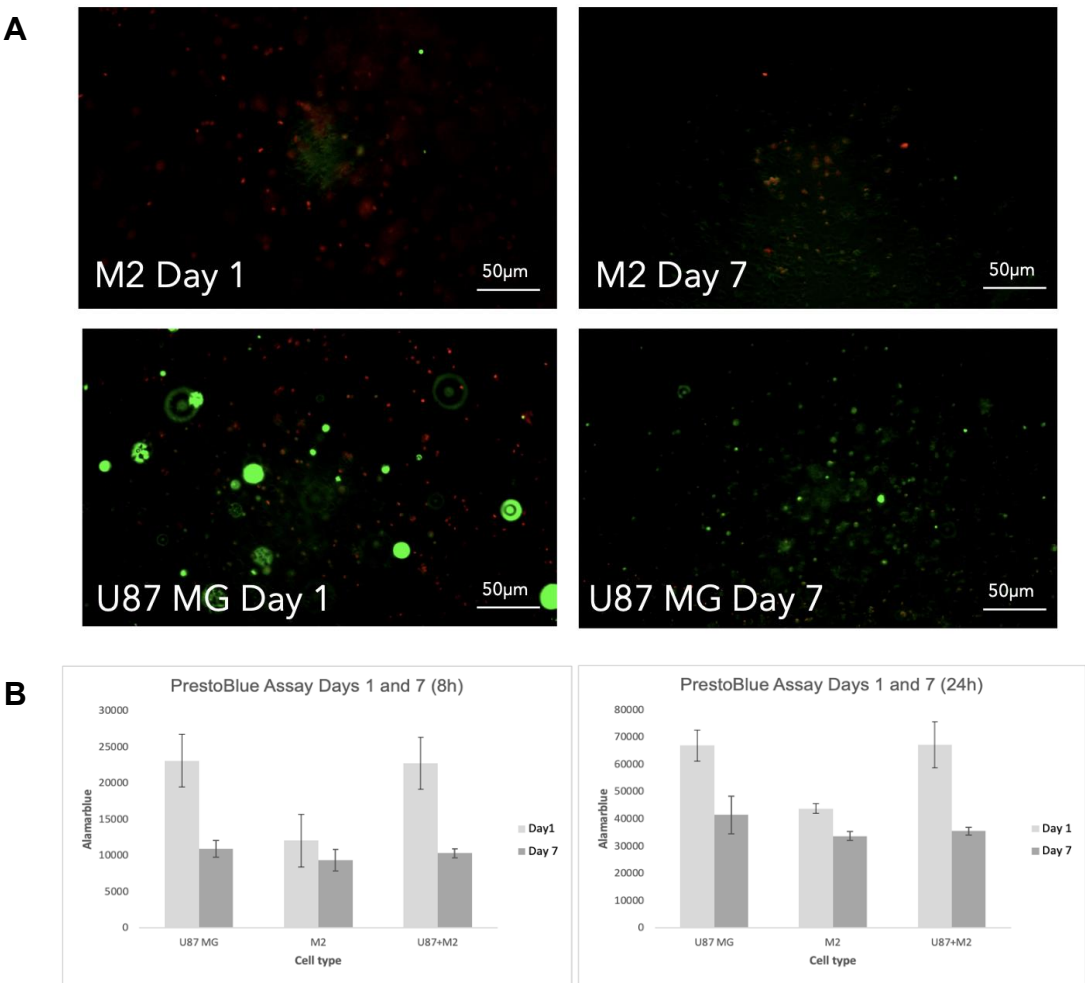

Figure 7. Live/Dead (cell viability) and PrestoBlue (proliferation) Assays for dopamine (DA) grafted HA-CS composite hydrogels. A) *Cell viability images of days 1 and 7 timepoints for M2-type cells and U87 MG cells.* ***B)*** *Cell proliferation graphs of days 1 and 7 timepoints for M2-type cells and U87 MG cells.*

We therefore carried out the biocompatibility studies with the HA-CS gels which were made by crosslinking CS-Ald and HA-CDH components, (excluding dopamine). This time, EDTA (2mM) was applied for 10 minutes to detach the primed and polarized THP-1 cells (M2-type macrophages). The cell viability of U87 MG cells appeared to improve with the use of HA-CDH when compared to the use of HA-DA-CDH in both days 1 and 7, as seen in Figure 8A. The PrestoBlue assay also showed signs of proliferation on U87 MG cells, increasing up to roughly 30% by day 7 (Figure 8B). The proliferation capability of THP-1 cells is lost once primed and polarized (Genin, Clement, Fattaccioli, Raes, & Michiels, 2015), therefore no proliferation signal was shown in M2-type cells as expected in the PrestoBlue assay. Anyhow, the Live/Dead assay showed a significant amount of live cells in both the time points (Figure 8B).

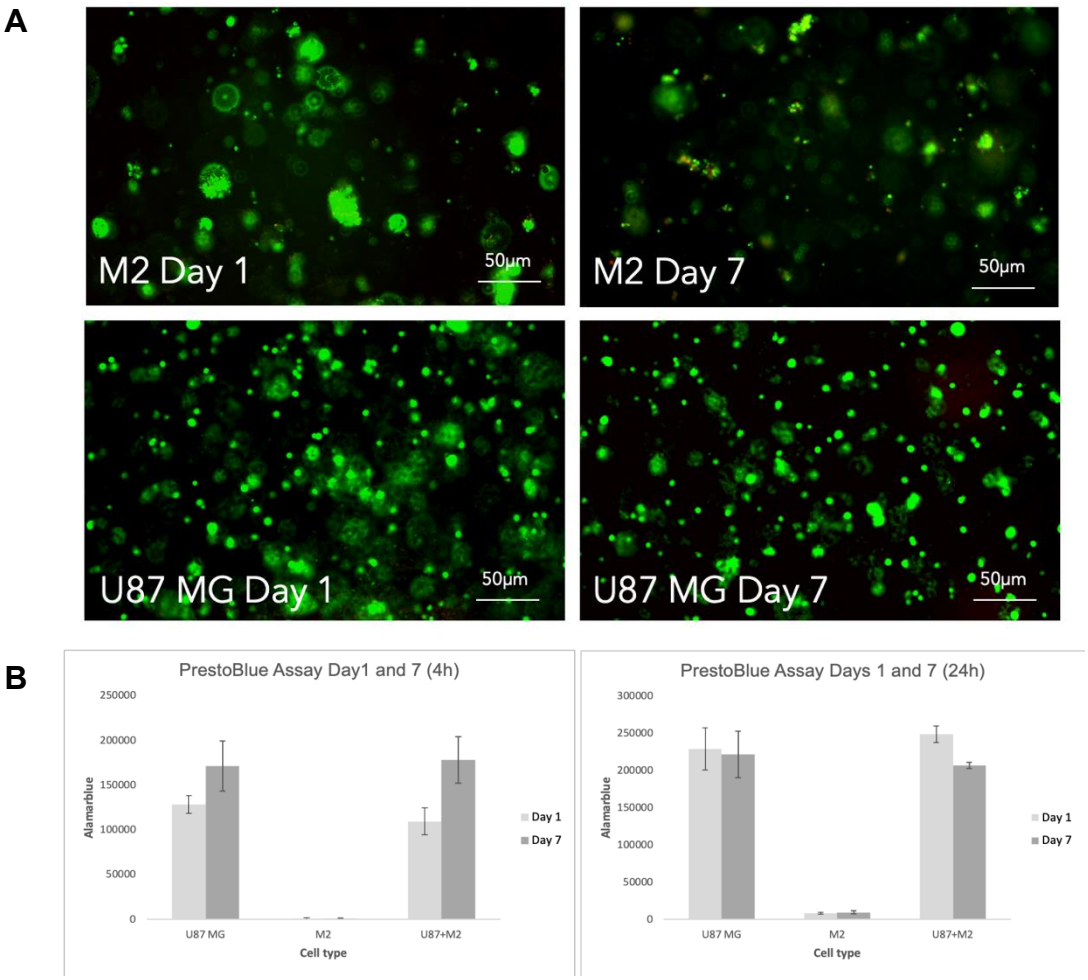

Figure 8. Live/Dead (cell viability) and PrestoBlue (proliferation) assays for HA-CS composite hydrogels. A) *Cell viability images of days 1 and 7 timepoints for M2-type cells and U87 MG cells.* ***B)*** *Cell proliferation graphs of days 1 and 7 timepoints for M2-type cells and U87 MG cells.*

Since good biocompatibility and cell viability results were obtained for both cell types, HA-CS hydrogel composite excluding DA was used to create a co-culture system between macrophages and glioblastoma cells, as seen in Figure 9C. We first studied the influence that THP-1 differentiated macrophages (M2-type) could have on U87 glioblastoma cells when co-cultured in the same hydrogel – in a glioblastoma microenvironment (GME).

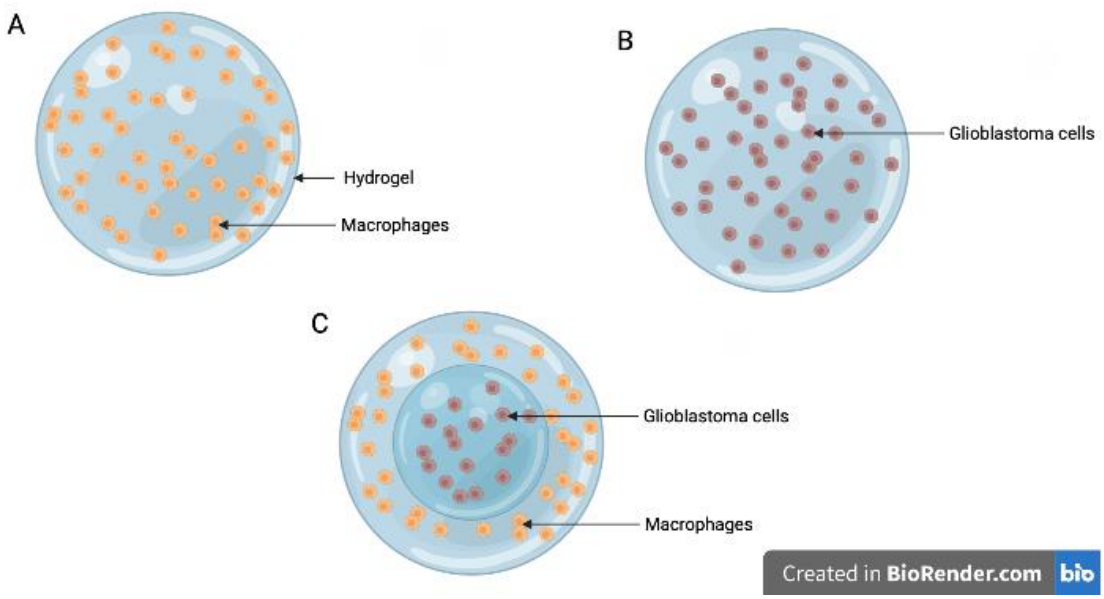

Figure 9. Schematic view of the three hydrogel groups. A) *Macrophage control group.* ***B)*** *Glioblastoma control group.* ***C)*** *Glioblastoma microenvironment co-culture group. Created with BioRender.com*

5.2 Gene Expression Analysis in Co-culture

Changes in gene expression were analysed from THP-1 differentiated macrophages (M2-type) and U87 glioblastoma cells co-cultured in the same HA-CS hydrogel composite. As controls, only the mentioned cell types were encapsulated in separate hydrogels. Brain-specific and immune-specific genes were analysed, which included: fibroblast growth factor 2 (FGF-2), matrix metallopeptidase (MMP-9), tumour necrosis factor (TNF), interleukin-1 receptor antagonist (IL-1RA), interleukin-10 (IL-10), mannose receptor C-type 1 (MRC-1), e-cadherin (CDH-1) and nestin (NES) (Table 1). The up- or down-regulation of these genes indicate the change in level of the cells' behaviour, such as tumour growth and cell survival capabilities, angiogenesis, cell migration, or anti-inflammatory properties, therefore stipulating the type of relationship and communication between macrophages and glioblastoma cells.

The GME hydrogels were first analysed after a week (Figure 10). These were collected, and the inner hydrogels containing the U87 MG cells were separated from the outer hydrogels containing the macrophages to later extract their RNA individually for further analysis. Later, average relative gene expression levels from the control hydrogel groups were compared to the relative gene expression levels in GME groups.

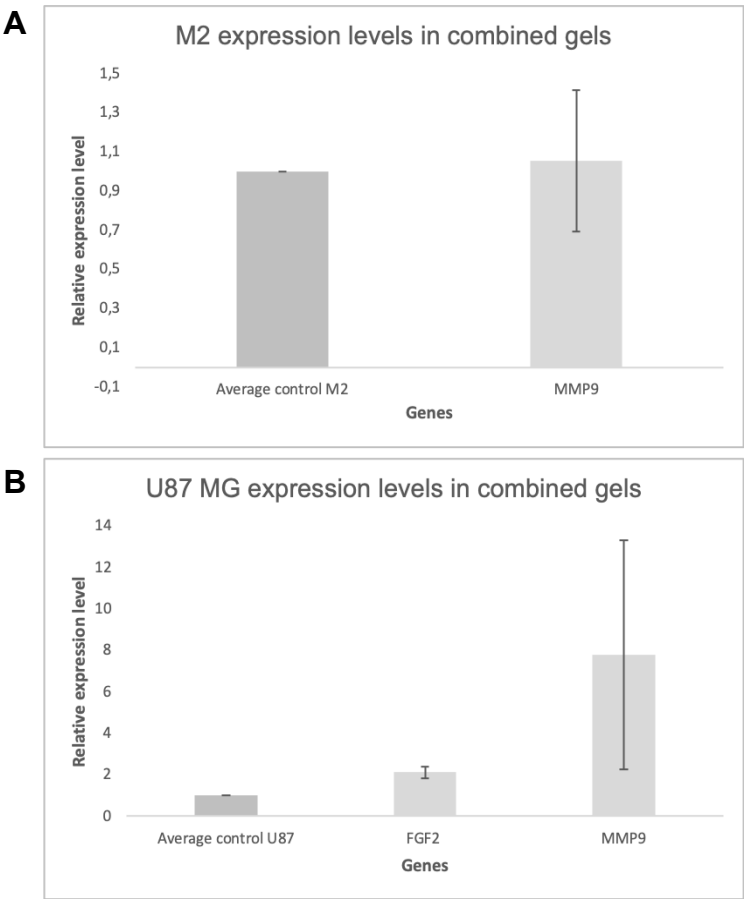

Figure 10. Gene expression of brain-specific (glioma) and immune-specific (macrophages) genes at day 7 timepoint. A) *Gene expressions of M2-type cells.* ***B)*** *Gene expressions of U87 MG cells.*

At first, the qRT-PCR data only estimated the expression of FGF-2 and MMP-9 genes for U87 MG cells, and only the MMP-9 gene expression was detected in the gels with M2-type cells (Figure 10). It could be noted that there was an increase in FGF-2 and MMP-9 gene expression levels in U87 MG cells in co-culture. This suggested that there was a cross-talk between macrophages and cancer cells, improving their cell survival, tumour growth and invasion (Li, Guo, Wang, Wang, & Li, 2020). Not enough gene expression data was obtained from the M2-type cells, but a slight increase in MMP-9 expression was seen. Thus, we conclude that one week of co-culturing was not long enough to obtain enough mRNA for the qRT-PCR study.

The GME setup was then repeated and analysed after two weeks. The qRT-PCR showed signal for all the analysed gene expressions for both U87 MG and M2-type cells (Figure 11).

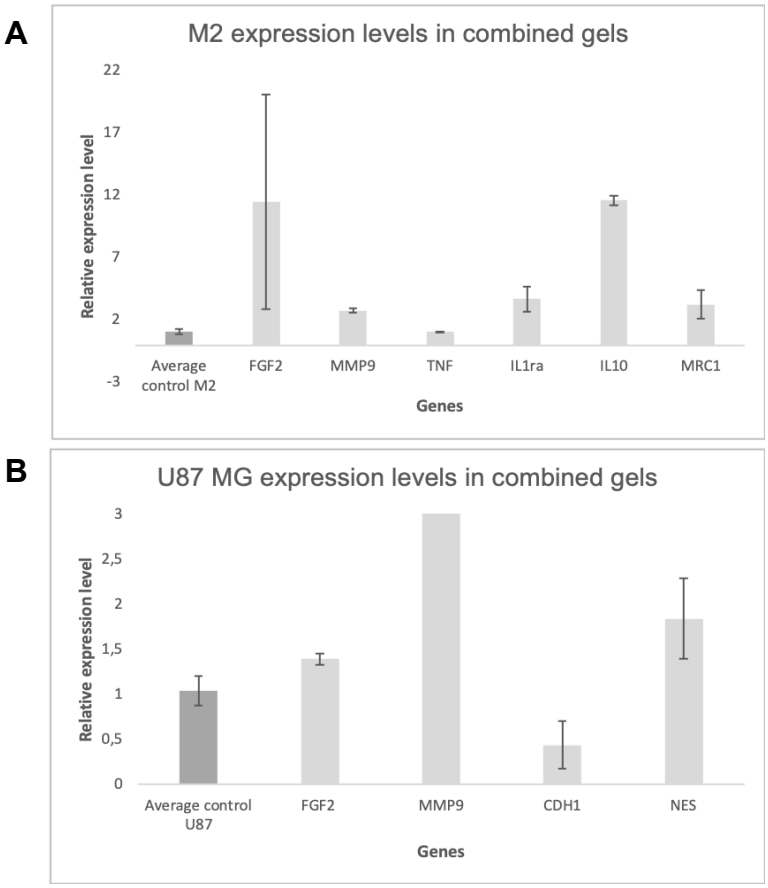

Figure 11. Gene expression of brain-specific (glioma) and immune-specific (macrophages) genes. A) *Gene expressions of M2-type cells.* ***B)*** *Gene expressions of U87 MG cells.*

Relative gene expression levels of most of the analysed genes appeared to change in the cells in the GME group in relation to the control hydrogels – when the cells were cultured individually – suggesting that when co-cultured, both U87 MG and M2-type cells underwent molecular changes, and there was therefore a cross-talk between the different cells. IL-10 and IL-1RA expression levels had a great increase in M2-type cells when co-cultured, having a greater anti-inflammatory effect (Iyer & Cheng, 2012). The upregulation of the MRC-1 gene in TAMs (Figure 11), also known as the CD206 marker, has been positively correlated with tumour cell proliferation and invasion (Haque et al., 2019). Upregulation of FGF-2 and MMP-9 in U87 MG cells was observed when co-cultured with macrophages, as seen in the previous experiment, but also NES relative expression level increased enhancing growth and invasiveness (Neradil & Veselska, 2015). Additionally, CDH-1 was found to be downregulated, enhancing the cancer cells' capabilities to migrate and grow (Liu & Chu, 2014).

It was noted that hydrogels started to degrade by day 14, so a 10-day timepoint was used for the following experiments. Moreover, we decided to execute the same model

with patient-derived primary glioma cells (BT-13). We decided to also use human blood-derived primary macrophages obtained from PBMC cells, differentiated into M1-type and M2-type macrophages to be analysed in the GME.

5.3 Use of Peripheral Blood Mononuclear Cells (PBMCs)

For the following experiments, THP-1 macrophages from PBMC cells and BT-13 cells were used. The PBMCs were polarized into both M1- and M2-type macrophages, which were then co-cultured separately with and without the presence of BT-13 cells. Then, qRT-PCR was carried out to analyse the cells' gene expressions after a 10-day timepoint in co-culture, having also control groups.

Figure 12 shows the relative gene expression levels when M1-type (Figure 11A) and M2-type (Figure 11B) macrophages were cultured together in a GME.

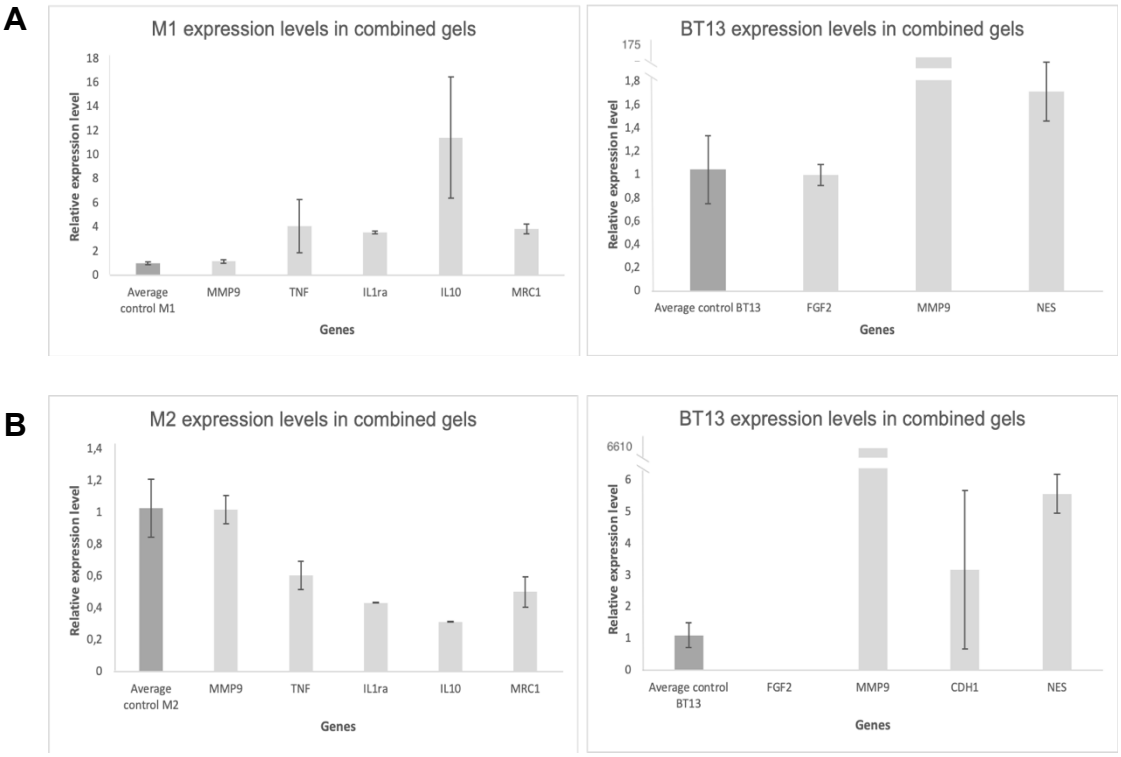

Figure 12. Gene expression of brain-specific (glioma) and immune-specific (macrophages) genes. A) *Gene expressions of M1-type and BT-13 cells.* ***B)*** *Gene expressions of M2-type and BT-13 cells.*

We could see that MMP-9, TNF, IL-1RA, IL-10 and MRC-1 genes in M1-type macrophages were upregulated relative to the control. These gene upregulations suggested that the presence of BT-13 cells was causing the M1-type macrophages to gain a TAM-like phenotype, becoming M2-type macrophages. Additionally, we observed that the M2-

type macrophages gene expressions were completely different from the results we previously obtained with the use of THP-1 M2-type macrophages and U87 MG cells, as this time MMP-9, TNF, IL-1RA, IL-10 and MRC-1 genes were downregulating, suggesting that the M2-type macrophages were gaining a similar phenotype to the one expected in M1-type macrophages, fighting against the tumour cells. We therefore decided to carry out the same experiment with the same cells, in order to compare with new results (Figure 13).

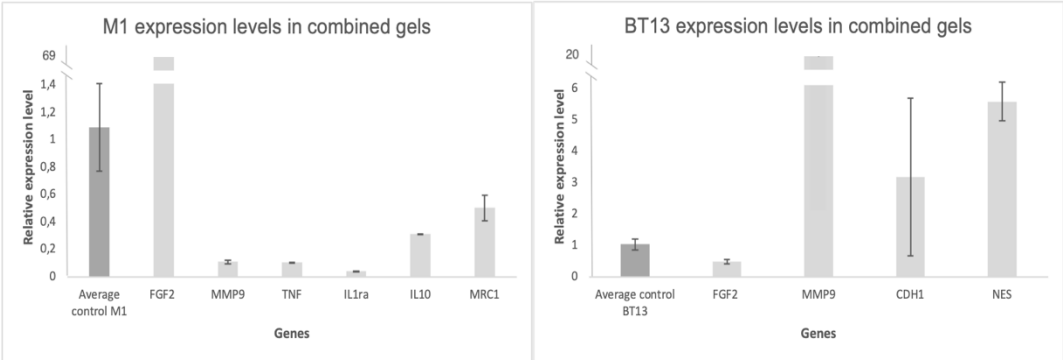

Figure 13. Gene expression of brain-specific (glioma) and immune-specific (macrophages) genes. *Gene expressions of M1-type and BT-13 cells.*

Unfortunately, sufficient mRNA expression was only obtained for the M1-type macrophages co-culture system (Figure 13). This could be due to the fact that hydrogels for the M2-type cells did not form correctly during the experimental procedure, and most of the M2-type and BT-13 cells were lost due to experimental error.

Interestingly, in this case the M1-type macrophages gene expression levels were downregulating (Figure 13) when compared to the previous results (Figure 12A). This time, the TNF gene – M1-type marker – downregulated when co-cultured with BT-13 cells, which met our expectations. In addition, the M2-type markers (IL-1RA, IL-10 and MRC-1) were expected to upregulate with the presence of BT-13 cells, and this behaviour could be seen in M1-type macrophages in figure 12A.

In addition, the decrease in relative expression level of FGF-2 in BT-13 cells (Figure 13) suggests that the cancer cells were indeed affected by the M1-type cells present in the hydrogel. The same happens with the apparent upregulation of CDH-1 in BT-13 cells, decreasing invasiveness and growth properties of cancer cells (Liu & Chu, 2014). On the other hand, these same BT-13 cells experienced an upregulation of the MMP-9 and NES genes, showing that their cancer progression and cell remodelling capabilities were not interfered by the presence of M1-type cells (Neradil & Veselska, 2015).

We also observed different gene expression levels in M2-type cells (Figure 12B). In previous results, M2-type cells had a greater anti-inflammatory effect (Figure 11) by the upregulation of IL-10 and IL-1RA genes (Iyer & Cheng, 2012). Also, the upregulation of MRC-1 gene enhanced cell-to-cell recognition and phagocytosis of immune cells (von Ehr et al., 2020). On the other hand, we later observed that most of the genes analysed in M2-type cells were downregulated (Figure 12B). A possible reason for this could be that the PBMCs did not differentiate completely into M2-type macrophages. Comparisons of M2-type macrophages with the use of PBMCs and BT-13 cells could not be done as gene expression data was not obtained.

6. CONCLUSION

In this project we created hydrogels to mimic the brain microenvironment with the use of common extracellular matrix (ECM) compounds, to analyse and evaluate the behaviour of glioblastoma cells and macrophages, to be studied as a possible *in vitro* model.

The results obtained during the project show that HA-CDH with CS-Ald hydrogels offer a favourable microenvironment for glioblastoma cells to grow and develop and offers a platform capable of sustaining macrophages. The combination of glioblastoma cells and macrophages in the designed *in vitro* model offered the possibility to analyse the cell's gene expressions, revealing the upregulation of genes such as FGF-2, IL-10 or MRC-1 in M2-type cells when plated together with glioblastoma cells, enhancing these cancer cells to proliferate – also shown by Ling Qi (Qi et al., 2016) in a study about the IL-10 secretion from M2-type cells. This designed model also demonstrated the downregulation of the same genes in M1-type cells in the presence of glioblastoma cells – as seen in a study about the crosstalk between microglia and glioblastoma by Jee-Wei Emily Chen (Chen et al., 2020) – inhibiting the cancer cells from taking advantage of the signalling pathways.

It has been demonstrated that the created hydrogel microenvironment gave reliable results with the use of THP-1 and U87 MG cell lines, but further studies need to be done with PBMCs and BT-13 primary cells to analyse more deeply their behaviour in a tumour-like microenvironment.

This hydrogel platform opens a wide range of possible research areas and applications, such as disease modelling combined with drug analyses and testing, or the use of nanoparticles to target and silence specific glioblastoma genes.

7. REFERENCES

Ade, C., Pum, J., Abele, I., Raggub, L., Bockmühl, D., & Zöllner, B. (2021). Analysis of cycle threshold values in SARS-CoV-2-PCR in a long-term study. *Journal of Clinical Virology*, *138*(December 2020), 2020–2022. https://doi.org/10.1016/j.jcv.2021.104791

Aswathy, S. H., Narendrakumar, U., & Manjubala, I. (2020). A Practical Guide to Hydrogels for Cell Culture Steven. *Heliyon*, *6*(4), e03719. https://doi.org/10.1016/j.heliyon.2020.e03719

Baghban, R., Roshangar, L., Jahanban-Esfahlan, R., Seidi, K., Ebrahimi-Kalan, A., Jaymand, M., … Zare, P. (2020). Tumor microenvironment complexity and therapeutic implications at a glance. *Cell Communication and Signaling*, *18*(1), 1–19. https://doi.org/10.1186/s12964-020-0530-4

Barriga, V., Kuol, N., Nurgali, K., & Apostolopoulos, V. (2019). The complex interaction between the tumor micro-environment and immune checkpoints in breast cancer. *Cancers*, *11*(8). https://doi.org/10.3390/cancers11081205

Bershteyn, M., & Kriegstein, A. R. (2013). Cerebral organoids in a dish: Progress and prospects. *Cell*, *155*(1), 19. https://doi.org/10.1016/j.cell.2013.09.010

Bignami, A., Hosley, M., & Dahl, D. (1993). Hyaluronic acid and hyaluronic acid-binding proteins in brain extracellular matrix. *Anatomy and Embryology*, *188*(5), 419–433. https://doi.org/10.1007/BF00190136

Blanco-Fernandez, B., Gaspar, V. M., Engel, E., & Mano, J. F. (2021). Proteinaceous Hydrogels for Bioengineering Advanced 3D Tumor Models. *Advanced Science*. https://doi.org/10.1002/advs.202003129

Catoira, M. C., Fusaro, L., Di Francesco, D., Ramella, M., & Boccafoschi, F. (2019). Overview of natural hydrogels for regenerative medicine applications. *Journal of Materials Science: Materials in Medicine*, *30*(10). https://doi.org/10.1007/s10856-019-6318-7

Chaicharoenaudomrung, N., Kunhorm, P., & Noisa, P. (2019). Three-dimensional cell culture systems as an in vitro platform for cancer and stem cell modeling. *World Journal of Stem Cells*, *11*(12), 1065–1083. https://doi.org/10.4252/wjsc.v11.i12.1065

Chen, J. W. E., Lumibao, J., Leary, S., Sarkaria, J. N., Steelman, A. J., Gaskins, H. R., & Harley, B. A. C. (2020). Crosstalk between microglia and patient-derived glioblastoma cells inhibit invasion in a three-dimensional gelatin hydrogel model. *Journal of Neuroinflammation*, *17*(1), 1–15. https://doi.org/10.1186/s12974-020-02026-6

Croft, C. L., Futch, H. S., Moore, B. D., & Golde, T. E. (2019). Organotypic brain

slice cultures to model neurodegenerative proteinopathies. *Molecular Neurodegeneration*, *14*(1), 1–11. https://doi.org/10.1186/s13024-019-0346-0

Desmond, J. P. and J. E. (2019). The role of the human cerebellum in performance monitoring. *Physiology & Behavior*, *176*(3), 139–148. https://doi.org/10.1016/j.conb.2016.06.011.The

Dingle, Y. T. L., Boutin, M. E., Chirila, A. M., Livi, L. L., Labriola, N. R., Jakubek, L. M., … Hoffman-Kim, D. (2015). Three-Dimensional Neural Spheroid Culture: An In Vitro Model for Cortical Studies. *Tissue Engineering - Part C: Methods*, *21*(12), 1274–1283. https://doi.org/10.1089/ten.tec.2015.0135

Edmondson, R., Broglie, J. J., Adcock, A. F., & Yang, L. (2014). Three-dimensional cell culture systems and their applications in drug discovery and cell-based biosensors. *Assay and Drug Development Technologies*, *12*(4), 207–218. https://doi.org/10.1089/adt.2014.573

El-Sherbiny, I. M., & Yacoub, M. H. (2013). Hydrogel scaffolds for tissue engineering: Progress and challenges. *Global Cardiology Science and Practice*, *2013*(3), 38. https://doi.org/10.5339/gcsp.2013.38

Elhelu, M. A. (1983). The role of macrophages in immunology. *Journal of the National Medical Association*, *75*(3), 314–317.

Fallacara, A., Baldini, E., Manfredini, S., & Vertuani, S. (2018). Hyaluronic acid in the third millennium. *Polymers*, *10*(7). https://doi.org/10.3390/polym10070701

Genin, M., Clement, F., Fattaccioli, A., Raes, M., & Michiels, C. (2015). M1 and M2 macrophages derived from THP-1 cells differentially modulate the response of cancer cells to etoposide. *BMC Cancer*, *15*(1), 1–14. https://doi.org/10.1186/s12885-015-1546-9

Gutschner, T., & Diederichs, S. (2012). The hallmarks of cancer: A long non-coding RNA point of view. *RNA Biology*, *9*(6), 703–719. https://doi.org/10.4161/rna.20481

Haimes, J., & Kelley, M. (2010). Demonstration of a ΔΔ C q Calculation Method to Compute Relative Gene Expression from qPCR Data. *GE Healthcare, Tech Note*, 1–4. Retrieved from http://dharmacon.gelifesciences.com/uploadedfiles/resources/delta-cq-solaris-technote.pdf

Hanif, F., Muzaffar, K., Perveen, K., Malhi, S. M., & Simjee, S. U. (2017). Glioblastoma multiforme: A review of its epidemiology and pathogenesis through clinical presentation and treatment. *Asian Pacific Journal of Cancer Prevention*, *18*(1), 3–9. https://doi.org/10.22034/APJCP.2017.18.1.3

Haque, A. S. M. R., Moriyama, M., Kubota, K., Ishiguro, N., Sakamoto, M., Chinju, A., … Nakamura, S. (2019). CD206+ tumor-associated macrophages promote proliferation and invasion in oral squamous cell

carcinoma via EGF production. *Scientific Reports*, *9*(1), 1–10. https://doi.org/10.1038/s41598-019-51149-1

Heinrich, M. A., Bansal, R., Lammers, T., Zhang, Y. S., Michel Schiffelers, R., & Prakash, J. (2019). 3D-Bioprinted Mini-Brain: A Glioblastoma Model to Study Cellular Interactions and Therapeutics. *Advanced Materials*, *31*(14), 1–9. https://doi.org/10.1002/adma.201806590

Henrotin, Y., Mathy, M., Sanchez, C., & Lambert, C. (2010). Chondroitin sulfate in the treatment of osteoarthritis: From in vitro studies to clinical recommendations. *Therapeutic Advances in Musculoskeletal Disease*, *2*(6), 335–348. https://doi.org/10.1177/1759720X10383076

Iyer, S. S., & Cheng, G. (2012). Role of interleukin 10 transcriptional regulation in inflammation and autoimmune disease. *Critical Reviews in Immunology*, *32*(1), 23–63. https://doi.org/10.1615/critrevimmunol.v32.i1.30

Jodat, Y. A., Kang, M. G., Kiaee, K., Kim, G. J., Martinez, F. H., Rosenkranz, A., … Biotechnology, R. (2019). Human-Derived Organ-on-a-Chip for Personalized Drug Development, *24*(45), 5471–5486. https://doi.org/10.2174/1381612825666190308150055.Human-Derived

Jorfi, M., D'Avanzo, C., Kim, D. Y., & Irimia, D. (2018). Three-Dimensional Models of the Human Brain Development and Diseases. *Advanced Healthcare Materials*, *7*(1), 1–36. https://doi.org/10.1002/adhm.201700723

Kačarević, Ž. P., Rider, P. M., Alkildani, S., Retnasingh, S., Smeets, R., Jung, O., … Barbeck, M. (2018). An introduction to 3D bioprinting: Possibilities, challenges and future aspects. *Materials*, *11*(11). https://doi.org/10.3390/ma11112199

Kapałczyńska, M., Kolenda, T., Przybyła, W., Zajączkowska, M., Teresiak, A., Filas, V., … Lamperska, K. (2018). 2D and 3D cell cultures – a comparison of different types of cancer cell cultures. *Archives of Medical Science*, *14*(4), 910–919. https://doi.org/10.5114/aoms.2016.63743

Koivusalo, L., Kauppila, M., Samanta, S., Parihar, V. S., Ilmarinen, T., Miettinen, S., … Skottman, H. (2019). Tissue adhesive hyaluronic acid hydrogels for sutureless stem cell delivery and regeneration of corneal epithelium and stroma. *Biomaterials*, *225*(September), 119516. https://doi.org/10.1016/j.biomaterials.2019.119516

Krebs, J.E., E.S. Goldstein, and S. T. K. (2017). *Lewin's GENES XI Jones & Barlett Learning*. *Encounters in Microbiology* (Vol. 1).

Lall, N., Henley-Smith, C. J., De Canha, M. N., Oosthuizen, C. B., & Berrington, D. (2013). Viability reagent, prestoblue, in comparison with other available reagents, utilized in cytotoxicity and antimicrobial assays. *International Journal of Microbiology*, *2013*, 1–5. https://doi.org/10.1155/2013/420601

Lee, J. H., & Kim, H. W. (2018). Emerging properties of hydrogels in tissue engineering. *Journal of Tissue Engineering*, *9*, 0–3.

https://doi.org/10.1177/2041731418768285

Lehmann, R., Lee, C. M., Shugart, E. C., Benedetti, M., Charo, R. A., Gartner, Z., … Wilson, K. M. (2019). Human organoids: A new dimension in cell biology. *Molecular Biology of the Cell*, *30*(10), 1129–1137. https://doi.org/10.1091/mbc.E19-03-0135

Li, Y., Guo, X. B., Wang, J. S., Wang, H. C., & Li, L. P. (2020). Function of fibroblast growth factor 2 in gastric cancer occurrence and prognosis. *Molecular Medicine Reports*, *21*(2), 575–582. https://doi.org/10.3892/mmr.2019.10850

Liaw, C. Y., Ji, S., & Guvendiren, M. (2018). Engineering 3D Hydrogels for Personalized In Vitro Human Tissue Models. *Advanced Healthcare Materials*, *7*(4). https://doi.org/10.1002/adhm.201701165

Liu, X., & Chu, K. M. (2014). E-cadherin and gastric cancer: Cause, consequence, and applications. *BioMed Research International*, *2014*, 1–9. https://doi.org/10.1155/2014/637308

Mansour, A. K., Eid, M. M., & Khalil, N. S. A. M. (2003). Synthesis and reactions of some new heterocyclic carbohydrazides and related compounds as potential anticancer agents. *Molecules*, *8*(10), 744–755. https://doi.org/10.3390/81000744

Mantha, S., Pillai, S., Khayambashi, P., Upadhyay, A., & Zhang, Y. (2019). Smart Hydrogels in Tissue Engineering and. *Materials*, *12*(3323), 33. Retrieved from https://www.ncbi.nlm.nih.gov/pmc/articles/PMC68/

Mitlöhner, J., Kaushik, R., Niekisch, H., Blondiaux, A., Gee, C. E., Happel, M. F. K., … Seidenbecher, C. (2020). Dopamine Receptor Activation Modulates the Integrity of the Perisynaptic Extracellular Matrix at Excitatory Synapses. *Cells*, *9*(2), 1–21. https://doi.org/10.3390/cells9020260

Neradil, J., & Veselska, R. (2015). Nestin as a marker of cancer stem cells. *Cancer Science*, *106*(7), 803–811. https://doi.org/10.1111/cas.12691

Neri, S., Mariani, E., Meneghetti, A., Cattini, L., & Facchini, A. (2001). Calcein-acetyoxymethyl cytotoxicity assay: Standardization of a method allowing additional analyses on recovered effector cells and supernatants. *Clinical and Diagnostic Laboratory Immunology*, *8*(6), 1131–1135. https://doi.org/10.1128/CDLI.8.6.1131-1135.2001

Pardoll, D. (2015). Cancer and Immune System: Basic Concepts and Targets for Intervention. *Seminars in Oncology*, *42*(4), 523–538. https://doi.org/10.1053/j.seminoncol.2015.05.003

Qi, L., Yu, H., Zhang, Y., Zhao, D., Lv, P., Zhong, Y., & Xu, Y. (2016). IL-10 secreted by M2 macrophage promoted tumorigenesis through interaction with JAK2 in glioma. *Oncotarget*, *7*(44), 71673–71685. https://doi.org/10.18632/oncotarget.12317

Rauch, U. (2004). Extracellular matrix components associated with remodeling processes in brain. *Cellular and Molecular Life Sciences*, *61*(16), 2031–2045. https://doi.org/10.1007/s00018-004-4043-x

Rauch, U., Feng, K., & Zhou, X. H. (2001). Neurocan: A brain chondroitin sulfate proteoglycan. *Cellular and Molecular Life Sciences*, *58*(12–13), 1842–1856. https://doi.org/10.1007/PL00000822

Ryu, N. E., Lee, S. H., & Park, H. (2019). Spheroid Culture System Methods and Applications for Mesenchymal Stem Cells. *Cells*, *8*(12), 1–13. https://doi.org/10.3390/cells8121620

Sachs, M. (1982). Anatomy of the brain. *Soins; La Revue de Reference Infirmiere*, *27*(2), 3–8.

Siemann, D. W. (2010). Tumor Microenvironment. *Tumor Microenvironment*. https://doi.org/10.1002/9780470669891

Suttkus, A., Morawski, M., & Arendt, T. (2016). Protective Properties of Neural Extracellular Matrix. *Molecular Neurobiology*, *53*(1), 73–82. https://doi.org/10.1007/s12035-014-8990-4

Tan, S. C., & Yiap, B. C. (2009). DNA, RNA, and protein extraction: The past and the present. *Journal of Biomedicine and Biotechnology*, *2009*. https://doi.org/10.1155/2009/574398

Tang, G., Zhou, B., Li, F., Wang, W., Liu, Y., Wang, X., … Ye, X. (2020). Advances of Naturally Derived and Synthetic Hydrogels for Intervertebral Disk Regeneration. *Frontiers in Bioengineering and Biotechnology*, *8*(June), 1–13. https://doi.org/10.3389/fbioe.2020.00745

Taylor, O. G., Brzozowski, J. S., & Skelding, K. A. (2019). Glioblastoma multiforme: An overview of emerging therapeutic targets. *Frontiers in Oncology*, *9*(SEP), 1–11. https://doi.org/10.3389/fonc.2019.00963

Troidl, C., Möllmann, H., Nef, H., Masseli, F., Voss, S., Szardien, S., … Elsässer, A. (2009). Classically and alternatively activated macrophages contribute to tissue remodelling after myocardial infarction. *Journal of Cellular and Molecular Medicine*, *13*(9 B), 3485–3496. https://doi.org/10.1111/j.1582-4934.2009.00707.x

Urbanska, K., Sokolowska, J., Szmidt, M., & Sysa, P. (2014). Glioblastoma multiforme - An overview. *Wspolczesna Onkologia*, *18*(5), 307–312. https://doi.org/10.5114/wo.2014.40559

Varghese, O. P., Wang, S., Oommen, O. P., & Yan, H. (2013). Mild and efficient strategy for site-selective aldehyde modification of glycosaminoglycans: Tailoring hydrogels with tunable release of growth factor. *Biomacromolecules*, *14*(7), 2427–2432. https://doi.org/10.1021/bm400612h

Volpi, N. (2019). Chondroitin sulfate safety and quality. *Molecules*, *24*(8). https://doi.org/10.3390/molecules24081447

von Ehr, A., Attaai, A., Neidert, N., Potru, P. S., Ruß, T., Zöller, T., & Spittau, B. (2020). Inhibition of Microglial TGFβ Signaling Increases Expression of Mrc1. *Frontiers in Cellular Neuroscience*, *14*(March), 1–10. https://doi.org/10.3389/fncel.2020.00066

Wang, H. W., & Joyce, J. A. (2010). Alternative activation of tumor-associated macrophages by IL-4: Priming for protumoral functions. *Cell Cycle*, *9*(24), 4824–4835. https://doi.org/10.4161/cc.9.24.14322

Wang, J., Li, D., Cang, H., & Guo, B. (2019). Crosstalk between cancer and immune cells: Role of tumor-associated macrophages in the tumor microenvironment. *Cancer Medicine*, *8*(10), 4709–4721. https://doi.org/10.1002/cam4.2327

Wang, M., Zhao, J., Zhang, L., Wei, F., Lian, Y., Wu, Y., … Guo, C. (2017). Role of tumor microenvironment in tumorigenesis. *Journal of Cancer*, *8*(5), 761–773. https://doi.org/10.7150/jca.17648

XiuJun (James) Li, Alejandra V. Valadez, Peng Zuo, and Z. N. (2012). Microfluidic 3D cell culture: potential application for tissue- based bioassays XiuJun, *4*(12), 1509–1525. https://doi.org/10.1016/j.earlhumdev.2006.05.022

Zhang, H., Wang, R., Yu, Y., Liu, J., Luo, T., & Fan, F. (2019). Glioblastoma treatment modalities besides surgery. *Journal of Cancer*, *10*(20), 4793–4806. https://doi.org/10.7150/jca.32475

Zhang, X., Liu, Q., Liao, Q., & Zhao, Y. (2017). Potential roles of peripheral dopamine in tumor immunity. *Journal of Cancer*, *8*(15), 2966–2973. https://doi.org/10.7150/jca.20850

Zhu, J., & Marchant, R. E. (2011). Design properties of hydrogel tissue-engineering scaffolds. *Expert Review of Medical Devices*, *8*(5), 607–626. https://doi.org/10.1586/erd.11.27